J|A|C|S
COMMUNICATIONS

Published on Web 11/09/2004

Understanding the Basis of Resistance in the Irksome Lys103Asn HIV-1 Reverse Transcriptase Mutant through Targeted Molecular Dynamics Simulations

Fátima Rodríguez-Barrios and Federico Gago
Departamento de Farmacología, Universidad de Alcalá, E-28871 Alcalá de Henares, Madrid, Spain
Received July 30, 2004; E-mail: federico.gago@uah.es

Rapid selection of resistant viruses is a well-known consequence of treating HIV-1 infections with current drugs, including the clinically important class of inhibitors of the enzyme reverse transcriptase (RT). The Lys103Asn (K103N) substitution in RT is a frequent escape mutation that is selected both in vitro and in vivo by numerous non-nucleoside RT inhibitors (NNRTIs)[1] and is also commonly seen in patients receiving highly active antiretroviral therapy.[2] Lys103 is located at the outer rim of the pocket where NNRTIs bind but is very seldom involved in direct interactions with the bound drugs.[3,4] Attempts to understand the molecular basis of resistance have made use of different techniques including X-ray crystallography[5] and theoretical calculations.[6] However, the structures of the complexes of several inhibitors with wild-type (wt) and K103N mutant RT have revealed, with one exception,[7] comparable binding modes and similar interactions with the enzyme in the bound state.[3,8] These experimental results probably account for the fact that attempts to correlate calculated interaction energies with experimental activities against the K103N mutant enzyme have met with only limited success.[9]

Formation of the NNRTI binding pocket requires rearrangement of structural elements located mainly between the β6-β10-β9 and β12-β13-β14 sheets of the p66 subunit (Figure 1). The unliganded enzyme adopts a closed conformation in which the p66 thumb subdomain folds down into the DNA binding cleft and makes contacts with the tip of the fingers.[10,11] Upon binding to either DNA template-primer or NNRTIs, the p66 thumb subdomain adopts an open conformation and, together with the p66 fingers and palm subdomain, forms a large cleft that accommodates the template-primer substrate.[12] The NNRTI binding pocket is located close to, but distant from, the substrate binding site and is primarily made up of Leu100, Lys101, Lys103, Val106, Thr107, Val108, Val179, Tyr181, Tyr188, Val189, Gly190, Phe227, Trp229, Leu234, and Tyr318 in p66.[13] The putative entrance to this binding cavity is located at the interface of the p66/p51 heterodimer and is primarily formed by Pro95, Leu100, Lys101, Lys103, Val179, and Tyr181 of p66.[13−15]

Interestingly, the prediction in an early study of unliganded wt-RT that the K103N mutation could lead to the formation of additional hydrogen bonds that are not present in the wt enzyme[15] was later experimentally confirmed by other authors.[3] The crystal structure of the K103N apoenzyme (PDB code 1HQE) indeed showed a hydrogen bond between the Asn103 and Tyr188 side chains, for which no equivalent exists in the wt RT structure, and additional interactions with two neighboring water molecules. Since this hydrogen bonding network was suggested to stabilize the closed-pocket form of the mutant enzyme in the unliganded state, it was reasoned that it could also interfere with NNRTI entry. We have tested this hypothesis by performing two sets of simulations on the whole wt and K103N RT heterodimers (987 residues in all) in which the closed-pocket form of each enzyme[16] (as taken from

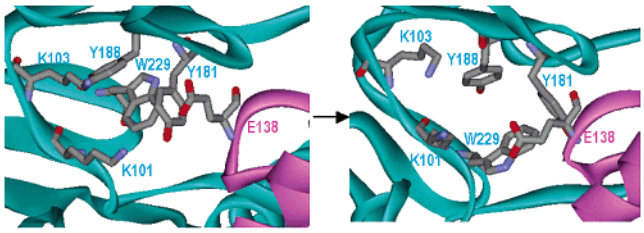

Figure 1. "Closed" (left) and "open" (right) conformations of the residues making up the NNRTI-binding pocket of wild-type HIV-1 RT (p66, cyan; p51, pink), as found in PDB entries 1DLO and 1BQM, respectively.

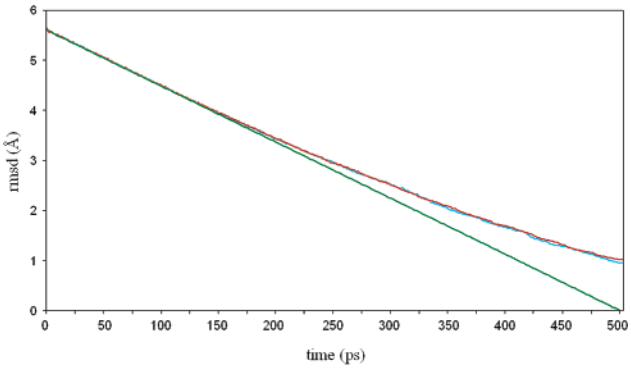

Figure 2. Time evolution of the mass-weighted root-mean-square deviation (rmsd) of all the atoms in the simulated structures compared to the reference structures (progression of the target rmsd value in green; actual values for wt- and K103N RT in cyan and red, respectively) when a force constant of 0.5 kcal mol^{-1} Å^{-2} was used.

PDB entries 1DLO[11] and 1HQE) was gradually forced to adopt the conformation of their NNRTI-bound counterparts (as taken from their respective complexes with the same inhibitor HBY097 [PDB codes 1BQM[17] and 1HQU[15]], upon removal of the ligand). A targeted molecular dynamics (tMD) approach,[18−20] as implemented in AMBER 7.0,[21] was used to apply a restraint force[22] onto each initial structure so as to bias the trajectories toward each respective target. The process of pocket creation started with the repositioning of the p66 thumb subdomain and was monitored by measuring the N−CA−CB−CG dihedral angles involving the side chains of Tyr181 and Tyr188, which are known to reorient by "flipping" toward the polymerase active site upon NNRTI binding[23] (Figure 1). A force constant of 0.125 kcal mol^{-1} Å^{-2} over 500 ps proved insufficient to reach the target structure (Supporting Information, Figure 1). Increasing this value to 0.25 (data not shown) or 0.5 kcal mol^{-1} Å^{-2} over the same period of time allowed a low-energy path to be found leading from the simulated structure to the target structure (Figure 2). It can be seen (Figure 3) that the two tyrosine side chains took longer to rearrange in the case of the K103N mutant enzyme, and the same result was obtained when the force constant was further increased to 1.0 kcal mol^{-1} Å^{-2} (Supporting Information, Figure 2). To check for possible protocol dependencies, three

10.1021/ja045409t CCC: $27.50

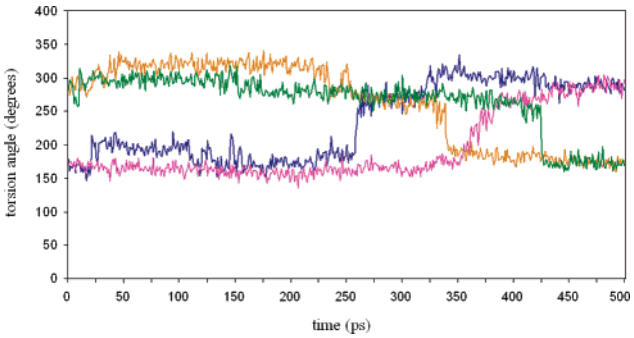

Figure 3. Time evolution of the N−CA−CB−CG dihedral angles of Y188 (blue, wt; magenta, K103N mutant) and Y181 (orange, wt; green, K103N mutant) side chains along the tMD simulation using a restraint force of 0.5 kcal mol^{-1} Å^{-2}.

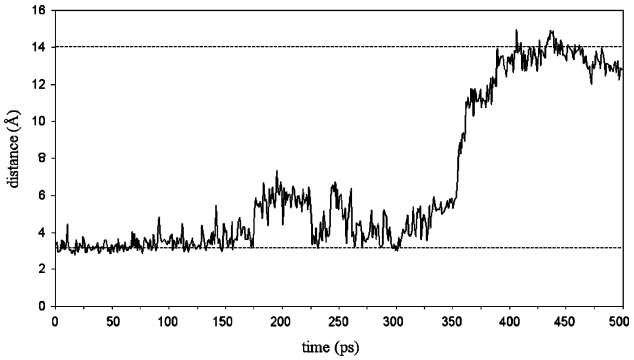

Figure 4. Time evolution of the distance between side chain atoms Nδ2 of Asn103 and OH of Tyr188. The broken lines represent the same distance as those found in the X-ray crystal structures of unliganded (bottom) and HBY097-bound (top) K103N RT.

additional simulations using the 0.5 kcal mol^{-1} Å^{-2} force constant were carried out in which the time span was set to 250 ps, 750 ps, and 1 ns (Supporting Information, Figure 3).

In all cases a consistent pattern arises showing that the closed form of the pocket where NNRTIs bind is indeed stabilized to a larger extent in the K103N mutant enzyme relative to wild-type. It is also seen that rearrangement of Tyr188 systematically precedes reorientation of Tyr181 and that, in the case of the K103N mutant, swinging of Tyr188 is closely coupled to the breaking of the hydrogen bond between this residue and Asn103 (Figure 4).

The demonstrated stabilization of the closed conformation of the RT structure could then interfere with NNRTI binding by imposing an extra energy barrier to the incoming inhibitor, which is in good accord with kinetic data. In fact, determination of the rate constants for nevirapine association with (k_{on}) and dissociation from (k_{off}) mutant and wt RT enzymes has shown that mutations L100I and V106A increase the k_{off} values 12- and 8.5-fold, respectively, without significantly affecting the k_{on}, whereas the K103N mutation decreases the k_{on} 5-fold without increasing the k_{off}.[24] Other mutations (e.g., Y181I and Y188L) conferring resistance to nevirapine can affect both k_{off} and k_{on} values.

The present results support the view that the primary resistance mechanism for the K103N mutation involves, at least to a large extent, a greater stabilization of the unbound state of HIV-1 RT relative to wt rather than a loss of interactions between the enzyme and the bound inhibitor (as seen for other mutants, e.g., Y181C and Y188L). Since this mechanism can interfere with inhibitor entry, the ensuing resistance is particularly worrying as it can conceivably affect many structural classes of NNRTIs irrespective of their molecular scaffolds. Nonetheless, some second-generation NNRTIs, e.g., capravirine and etravirine (formerly known as TMC-125), do have similar inhibitory efficacies against wild-type and the K103N RT mutant.[25] This finding means that these molecules are somehow able to overcome the energetic cost incurred on disrupting the hydrogen bonding network during the cavity creation process that leads to drug binding. Attempts to understand this behavior in atomic detail are currently underway.

Acknowledgment. Dedicated to the memory of the late Dr. Paul A. J. Janssen. F.R.-B. is a fellow of the Spanish Ministerio de Ciencia y Tecnología. Financial support from the Spanish CICYT (SAF2003-7219-C02), the European Commission (QLRT-2000-30291), and the National Foundation for Cancer Research is gratefully acknowledged.

Supporting Information Available: Eight additional figures (4 pages, print/PDF) showing the results of alternative simulation protocols and relevant NNRTI structures (PDF), and a Chime animation. This material is available free of charge via the Internet at http://pubs.acs.org.

References

(1) Silvestri, R.; De Martino, G.; La Regina, G.; Artico, M.; Massa, S.; Vargiu, L.; Mura, M.; Loi, A. G.; Marceddu, T.; La Colla, P. *J. Med. Chem.* **2003**, *46*, 2482−2493.
(2) Schinazi, R. F.; Larder, B. A.; Mellors, J. W. *Int. Antiviral News* **1997**, *5*, 129−135.
(3) Hsiou, Y.; Ding, J.; Das, K.; Clark, A. D., Jr.; Boyer, P. L.; Lewi, P.; Janssen, P. A. J.; Kleim, J. P.; Rösner, M.; Hughes, S. H.; Arnold, E. *J. Mol. Biol.* **2001**, *309*, 437−445.
(4) Rodríguez-Barrios, F.; Pérez, C.; Lobatón, E.; Velázquez, S.; Chamorro, C.; San-Félix, A.; Pérez-Pérez, M. J.; Camarasa, M. J.; Pelemans, H.; Balzarini, J.; Gago, F. *J. Med. Chem.* **2001**, *44*, 1853−1865.
(5) Ren, J.; Nichols, C. E.; Chamberlain, P. P.; Weaver, K. L.; Short, S. A.; Stammers, D. K. *J. Mol. Biol.* **2004**, *336*, 569−578.
(6) Rodríguez-Barrios, F.; Gago, F. *J. Am. Chem. Soc.* **2004**, *126*, 2718−2719.
(7) Ren, J.; Milton, J.; Weaver, K. L.; Short, S. A.; Stuart, D. I.; Stammers, D. K. *Struct. Fold. Des.* **2000**, *8*, 1089−1094.
(8) Lindberg, J.; Sigurösson, S.; Lowgren, S.; Andersson, H. O.; Sahlberg, C.; Noréen, R.; Fridborg, K.; Zhang, H.; Unge1, T. *Eur. J. Biochem.* **2002**, *6*, 1670−1677.
(9) Udier-Blagovic, M.; Watkins, E. K.; Tirado-Rives, J.; Jorgensen, W. L. *Bioorg. Med. Chem.* **2003**, *13*, 3337−3340.
(10) Rodgers, D. W.; Gamblin, S. J.; Harris, B. A.; Ray, S.; Culp, J. S.; Hellmig, B.; Woolf, D. J.; Debouck, C.; Harrison, S. C. *Proc. Natl. Acad. Sci. U.S.A.* **1995**, *92*, 1222−1226.
(11) Hsiou, Y.; Ding, J.; Das, K.; Clark, A. D., Jr.; Hughes, S. H.; Arnold, E. *Structure* **1996**, *4*, 853−860.
(12) (a) Jacobo-Molina, A.; Ding, J.; Nanni, R. G.; Clark, A. D., Jr.; Lu, X.; Tantillo, C.; Williams, R. L.; Kamer, G.; Ferris, A. L.; Clark, P.; Hizi, A.; Hughes, S. H.; Arnold, E. *Proc. Natl. Acad. Sci. U.S.A.* **1993**, *90*, 6320−6324. (b) Huang, H.; Chopra, R.; Verdine, G. L.; Harrison, S. C. *Science* **1998**, *282*, 1669−1675.
(13) Ding, J.; Das, K.; Tantillo, C.; Zhang, W.; Clark, A. D., Jr.; Jessen, S.; Lu, X.; Hsiou, Y.; Jacobo-Molina, A.; Andries, K.; Pauwels, R.; Moereels, H.; Koymans, L.; Janssen, P. A. J.; Smith, R.; Koepke, M. K.; Michejda, C.; Hughes, S. H.; Arnold, E. *Structure* **1995**, *3*, 365−379.
(14) Esnouf, R. M.; Ren, J.; Hopkins, A. L.; Ross, C. K.; Jones, E. Y.; Stammers, D. K.; Stuart, D. I. *Proc. Natl. Acad. Sci. U.S.A.* **1997**, *94*, 3984−3989.
(15) Ren, J.; Esnouf, R.; Garman, E.; Somers, D.; Ross, C.; Kirby, I.; Keeling, J.; Darby, G.; Jones, Y.; Stuart, D.; Stammers, D. *Nat. Struct. Biol.* **1995**, *2*, 293−302.
(16) A spherical shell of ∼210 TIP3P water molecules centered around the NNRTI binding pocket was used to solvate each system which was then heated and equilibrated at 300 K for 100 ps prior to the tMD simulation at the same temperature.
(17) Hsiou, Y.; Das, K.; Ding, J.; Clark, A. D., Jr; Kleim, J. P.; Rosner, M.; Winkler, I.; Riess, G.; Hughes, S. H.; Arnold, E. *J. Mol. Biol.* **1998**, *284*, 313−323.
(18) McCammon, J. A.; Karplus, M. *Proc. Natl. Acad. Sci. U.S.A.* **1997**, *76*, 3585−3592.
(19) Ma, J.; Karplus, M. *Proc. Natl. Acad. Sci. U.S.A.* **1997**, *94*, 11905−11910.
(20) Mendieta, J.; Gago, F. *J. Mol. Graphics Modell.* **2004**, *23*, 189−198.
(21) http://amber.scripps.edu/doc7/amber7.pdf.
(22) The force was defined in terms of a mass-weighted root-mean-square (rms) superposition to the final reference structure (target). The energy term has the following form: $E = 0.5k_rN(\text{rmsd} - \text{trmsd})^2$, where k_r is the force constant, N is the number of atoms, and trmsd is the target rms deviation which was set to zero.
(23) Jacobo-Molina, A.; Ding, J.; Nanni, R. G.; Clark, A. D., Jr.; Lu, X.; Tantillo, C.; Williams, R. L.; Kamer, G.; Ferris, A. L.; Clark, P.; Hizi, A.; Hughes, S. H.; Arnold, E. *Proc. Natl. Acad. Sci. U.S.A.* **1993**, *90*, 6320−6324.
(24) Maga, G.; Amacker, M.; Ruel, N.; Hübscher, U.; Spadari, S. *J. Mol. Biol.* **1997**, *274*, 738−747.
(25) Balzarini, J. Personal communication.

JA045409T